GATOR2 complex–mediated amino acid signaling regulates brain myelination

Zongyan Yu[a,b,c], Zhiwen Yang[b,c], Guoru Ren[b,c], Yingjie Wang[b,c], Xiang Luo[a,c], Feiyan Zhu[b,c], Shouyang Yu[d], Lanlan Jia[d], Mina Chen[d], Paul F. Worley[e,1], and Bo Xiao[b,c,1]

[a]School of Life Science and Technology, Harbin Institute of Technology, Harbin 150000, People's Republic of China; [b]Shenzhen Key Laboratory of Gene Regulation and Systems Biology, School of Life Sciences, Southern University of Science and Technology, Shenzhen 518005, People's Republic of China; [c]Department of Biology, School of Life Sciences, Brain Research Center, Southern University of Science and Technology, Shenzhen 518000, People's Republic of China; [d]Neuroscience & Metabolism Research, State Key Laboratory of Biotherapy, West China Hospital, Sichuan University and Collaborative Innovation Center, Chengdu 610041, People's Republic of China; and [e]The Solomon H. Snyder Department of Neuroscience, Johns Hopkins University School of Medicine, Baltimore, MD 21205

Edited by Jonah Chan, Department of Neurology, University of California, San Francisco, CA; received June 13, 2021; accepted November 16, 2021 by Editorial Board Member Jeremy Nathans

Amino acids are essential for cell growth and metabolism. Amino acid and growth factor signaling pathways coordinately regulate the mechanistic target of rapamycin complex 1 (mTORC1) kinase in cell growth and organ development. While major components of amino acid signaling mechanisms have been identified, their biological functions in organ development are unclear. We aimed to understand the functions of the critically positioned amino acid signaling complex GAP activity towards Rags 2 (GATOR2) in brain development. GATOR2 mediates amino acid signaling to mTORC1 by directly linking the amino acid sensors for arginine and leucine to downstream signaling complexes. Now, we report a role of GATOR2 in oligodendrocyte myelination in postnatal brain development. We show that the disruption of GATOR2 complex by genetic deletion of meiosis regulator for oocyte development (*Mios,* encoding a component of GATOR2) selectively impairs the formation of myelinating oligodendrocytes, thus brain myelination, without apparent effects on the formation of neurons and astrocytes. The loss of *Mios* impairs cell cycle progression of oligodendrocyte precursor cells, leading to their reduced proliferation and differentiation. *Mios* deletion manifests a cell type–dependent effect on mTORC1 in the brain, with oligodendroglial mTORC1 selectively affected. However, the role of *Mios*/GATOR2 in oligodendrocyte formation and myelination involves mTORC1-independent function. This study suggests that GATOR2 coordinates amino acid and growth factor signaling to regulate oligodendrocyte myelination.

myelination | oligodendrocytes | *Mios* | GATOR2 | amino acid signaling

Brain myelination is essential for the formation of functional neural circuitry in postnatal brain development (1). During the postnatal development, axons of brain neurons are wrapped with myelin sheath/membrane (rich in phospholipid and myelin protein) extended from oligodendrocytes. The myelin sheath facilitates fast conduction of nerve impulses along axons, which is required for neuronal processing and integration of information encoded in nerve impulses. Deficit in oligodendrocyte formation and myelination is implicated in neurological and psychiatric diseases (2, 3).

Myelination starts with the commitment of neural stem cells to the oligodendrocyte lineage, the formation of oligodendrocyte precursor cells (OPCs). OPCs divide several rounds before exiting the cell cycle and become postmitotic oligodendrocytes that further mature to myelin-forming oligodendrocytes (4, 5). This process involves extensive growth of oligodendrocyte processes, which demands synthesis of large amounts of biomaterial (e.g., myelin membrane). How the formation of the oligodendrocyte lineage and subsequent myelination are regulated remains incompletely understood. Previous studies have established that cell growth (increase in cell mass), proliferation, and differentiation of the oligodendrocyte lineage are regulated by growth factors that signal through protein kinase B (PKB/AKT), tuberous sclerosis complex (TSC), and ras homologue enriched in brain (Rheb) to mTORC1 (mechanistic target of rapamycin complex 1) kinase complex (6–11). mTORC1 is a master regulator of cellular metabolism, including protein and lipid synthesis (12). Therefore, mTORC1 plays an important role in tissue/organ growth and development.

Tissue/organ growth and development are dependent on the availability of nutrients, in particular amino acids (13, 14), which support cell growth in mass and proliferation (14). Nutrient supply is critically required for the formation of neural tissues (15), and early nutrition influences developmental myelination and cognition in infants and young children (16). The past decade has also seen an enormous progress toward biochemical understanding of amino acid sensing/signaling pathways (17), but the biological functions of amino acid sensing/signaling pathways in tissue growth and development are unknown. We aimed to examine the amino acid signaling pathways that regulate oligodendrocyte formation and myelination in coordination with growth factor signaling.

Significance

Fast transmission of nerve impulses with energetic efficiency along axons of nerve cells is essential for brain function. Toward this goal, axons are wrapped by the myelin membranes extended from oligodendrocytes, which is known as myelination of axons. Therefore, myelination is dependent on the formation of oligodendrocyte lineage cells. How the oligodendrocyte lineage is formed remains incompletely known. Previous studies suggest that signaling pathways of growth factors and amino acids might coordinate the regulation of oligodendrocyte formation, but the specific amino acid signaling pathway that participates in this regulation has not been identified. This study identifies the amino acid signaling complex GATOR2 (GAP activity towards Rags 2) as a positive regulator of oligodendrocyte formation and myelination that coordinately regulates brain myelination with growth factor signaling.

Author contributions: Z. Yu, P.F.W., and B.X. designed research; Z. Yu., Z. Yang, G.R., Y.W., X.L., F.Z., S.Y., and M.C. performed research; G.R. and L.J. contributed new reagents/analytic tools; Z. Yu, Z. Yang, Y.W., and X.L. analyzed data; and Z. Yu and B.X. wrote the paper.

The authors declare no competing interest.

This article is a PNAS Direct Submission. J.C. is a guest editor invited by the Editorial Board.

[1]To whom correspondence may be addressed. Email: pworley@jhmi.edu or xiaob@sustech.edu.cn.

This article contains supporting information online at http://www.pnas.org/lookup/suppl/doi:10.1073/pnas.2110917119/-/DCSupplemental.

Published January 12, 2022.

Studies of amino acid signaling pathways have been centered on the conserved lysosome-based GATOR (GAP activity towards Rags)–Rag pathway. Being conserved from the single-cell organism yeast (18) to metazoans (19), the GATOR–Rag pathway is involved in sensing multiple amino acids (20–23). In the presence of sufficient amounts of amino acids, recombination activating gene (Rag, a heterodimeric GTPase complex, RagA/B and RagC/D) recruits/anchors Raptor containing mTORC1 kinase complex to the surface of the lysosome (24, 25), where mTORC1 is activated by the growth factor–stimulated TSC/Rheb axis (26). Rag GTPase is regulated by GATOR1 (composed of DEPDC5, NPRL2, and NPRL3) and its upstream GATOR2 complex [composed of Mios, WDR24, WDR59, SEH1L, and SEC13 (27)]. GATOR1 inhibits Rag GTPase, while GATOR2 suppresses the inhibitory function of GATOR1 (GTPase activating protein) toward Rag GTPase. Therefore, GATOR2 functions upstream of GATOR1 as an activator of mTORC1 in amino acid signaling (22, 27).

To examine the role of amino acid signaling in brain development, we asked how disrupting GATOR2 function would affect oligodendrocyte myelination in the brain because GATOR2 is a critical link between amino acid sensors and the downstream protein complex signaling to mTORC1. Studies of heterologous cells and *Drosophila* predict that genetic knockout of the GATOR2 component Mios in the mouse would disrupt GATOR function, resulting in the reduction of mTORC1 activity (27, 28). We generated *Mios* genetic conditional knockout (cKO) mice and found in surprise that *Mios* cKO in neural stem cells and their progeny affects mTORC1 signaling in a cell type–dependent manner and that *Mios* cKO selectively impairs the formation of the oligodendrocyte lineage and brain myelination, without apparent effects on the formation of neurons and astrocytes. The finding identifies GATOR2 as an important positive regulator of oligodendrocyte formation and myelination. In addition, we show that GATOR2 plays a role in coordinate regulation of oligodendrocyte myelination by amino acid and growth factor signaling pathways.

Results

Mios Deletion in Neural Stem Cells Selectively Affects the Oligodendrocyte Lineage. Mios, an evolutionarily conserved protein, contains multiple WD40 protein–protein interaction repeats, as illustrated (*SI Appendix*, Fig. S1*A*). It is widely expressed in the mouse tissues (*SI Appendix*, Fig. S1*B*). In the brain, *Mios* is expressed in neurons and glia (oligodendrocytes and astrocytes), with more abundance in neurons (*SI Appendix*, Fig. S1*C*). To understand the physiological functions of the Mios-containing GATOR2 complex in vivo, we generated the floxed *Mios* (*Mios f/f*) mouse (*SI Appendix*, Fig. S1*D*). Germline deletion of *Mios* caused embryonic lethality around embryonic day 9. Conditional deletion of *Mios* (*Mios* cKO) in neural stem cells with *Nestin-Cre* (29) driver yielded offspring in Mendelian ratios, and the offspring with *Mios* homozygous knockout grew with normal body weight gain. Western blotting of the adult brain showed a drastic reduction in Mios protein, confirming a robust *Mios* deletion in neural cells of the brain (*SI Appendix*, Fig. S1 *E* and *F*). Albeit being slightly reduced in size, the *Mios* cKO brain was largely comparable with that of the normal control in gross anatomical structures (*SI Appendix*, Fig. S1 *G* and *H*). Histological examination of the cellular composition of the brain revealed that the formation of neurons and astrocytes in the *Mios f/f; Nestin-Cre* mouse appeared normal (*SI Appendix*, Fig. S1 *I–N*); however, the formation of the oligodendrocyte lineage was significantly impaired, as indicated by the assessment of oligodendrocyte lineage markers Olig2 and Sox10 (30). We found that the number of $Olig2^+$ $Sox10^+$ $DAPI^+$(4',6-diamidino-2-phenylindole) cells was significantly reduced in the corpus callosum of the *Mios f/f; Nestin-Cre* mouse (Fig. 1 *A* and *B*). In addition, brain myelination was significantly impaired; Black Gold staining and Luxol Fast Blue staining each showed reduced staining in gray and white matter of the forebrain of the *Mios f/f; Nestin-Cre* mouse (Fig. 1 *C* and *D*), indicating hypomyelination in the brain. Antibody staining of myelin oligodendrocyte glycoprotein (MOG) and myelin basic protein (MBP) also revealed reduced intensity of staining in the corpus callosum and cortex (Fig. 1 *E* and *F*). Western blotting and qRT-PCR further showed that the protein and messenger RNA (mRNA) levels related to multiple myelin proteins were reduced in the cortex and hippocampus (Fig. 1 *G–I*). All these findings suggest that deletion of *Mios* in neural stem cells selectively affects oligodendrocyte formation and myelination in the brain.

Mios Regulates Oligodendrocyte Myelination in an Oligodendrocyte-Intrinsic Manner. The selective effect of *Mios* deletion on the oligodendrocyte lineage prompted us to examine if the effect of *Mios* cKO on brain myelination is oligodendrocyte intrinsic. Toward this goal, we genetically deleted *Mios* in the OPCs (*Olig2-cre*) (31) and examined how oligodendrocyte myelination in the brain is affected. We found that deletion of *Mios* in OPCs (*Mios f/f; Olig2-Cre*) recapitulated the myelination deficit noted in the brain of the *Mios f/f; Nestin-Cre* mouse, as indicated by reduced intensity of Black Gold and MBP staining in the corpus callosum and cortex (Fig. 2 *A* and *B*) and reduced expressions of myelin genes and proteins in the cortex and hippocampus (Fig. 2 *C–E*). Electron microscopy (EM) showed that the number of unmyelinated axons in the optic nerve of the 4-wk *Mios f/f*; *Olig2*-Cre mouse was increased to 50% compared with 15% in the control mouse (Fig. 2 *F* and *G*), highlighting a developmental hypomyelination. The myelination deficit in the *Mios* cKO mouse persists to adulthood; EM revealed that in the 10-wk *Mios f/f; Olig2-Cre* mouse, the unmyelinated axons in the optic nerves still account for 30% vs. 10% in the control mouse (Fig. 2 *F* and *G*). Additionally, in the corpus callosum, the number of unmyelinated axons was increased to 70%, relative to 30% in the age-matched control (*SI Appendix*, Fig. S2 *A* and *B*). In addition, the g ratio of the myelinated axons in the optic nerve of the *Mios* cKO mouse was significantly increased, indicative of a reduction in the thickness of the myelin wraps (Fig. 2*H*). The average diameters of unmyelinated and myelinated axons in the optic nerve of the 4-wk *Mios* cKO mouse were comparable with those of the control mice, and the distributions of axon diameters in the optic nerves of the *Mios* cKO and control mice were similar, which suggest no axon degeneration/loss in the *Mios* cKO brain (*SI Appendix*, Fig. S2 *C* and *D*). Reduced Black Gold staining intensity and myelin protein expressions were apparent even in the 6-mo mouse (*SI Appendix*, Fig. S1 *E–G*). At this time point, *Mios* cKO mice did not exhibit apparent abnormalities in motor coordination and general activity levels/gross motor activity (*SI Appendix*, Fig. S2 *H* and *I*). All these findings indicate that Mios in oligodendroglia plays a cell-intrinsic role in regulating developmental myelination and that the loss of *Mios* causes persistent hypomyelination to adulthood.

Then, we asked if the effect of *Mios* cKO on myelination is region specific. We addressed this question using western blotting to assess myelin protein reduction in multiple brain regions (including the cortex, hippocampus, optic nerve, striatum, and cerebellum). The data show consistent reductions in myelin proteins in all these regions (*SI Appendix*, Fig. S3 *A* and *B*), albeit with varying degrees to each individual myelin protein. Likewise, MBP staining shows reduced intensity of myelinated fibers in the cortex and cerebellum of the *Mios* cKO mouse (*SI Appendix*, Fig. S3 *C* and *D*). Therefore, the hypomyelination is widespread in the brain of the *Mios* cKO mouse, which supports the notion that the amino acid sensing in oligodendrocyte

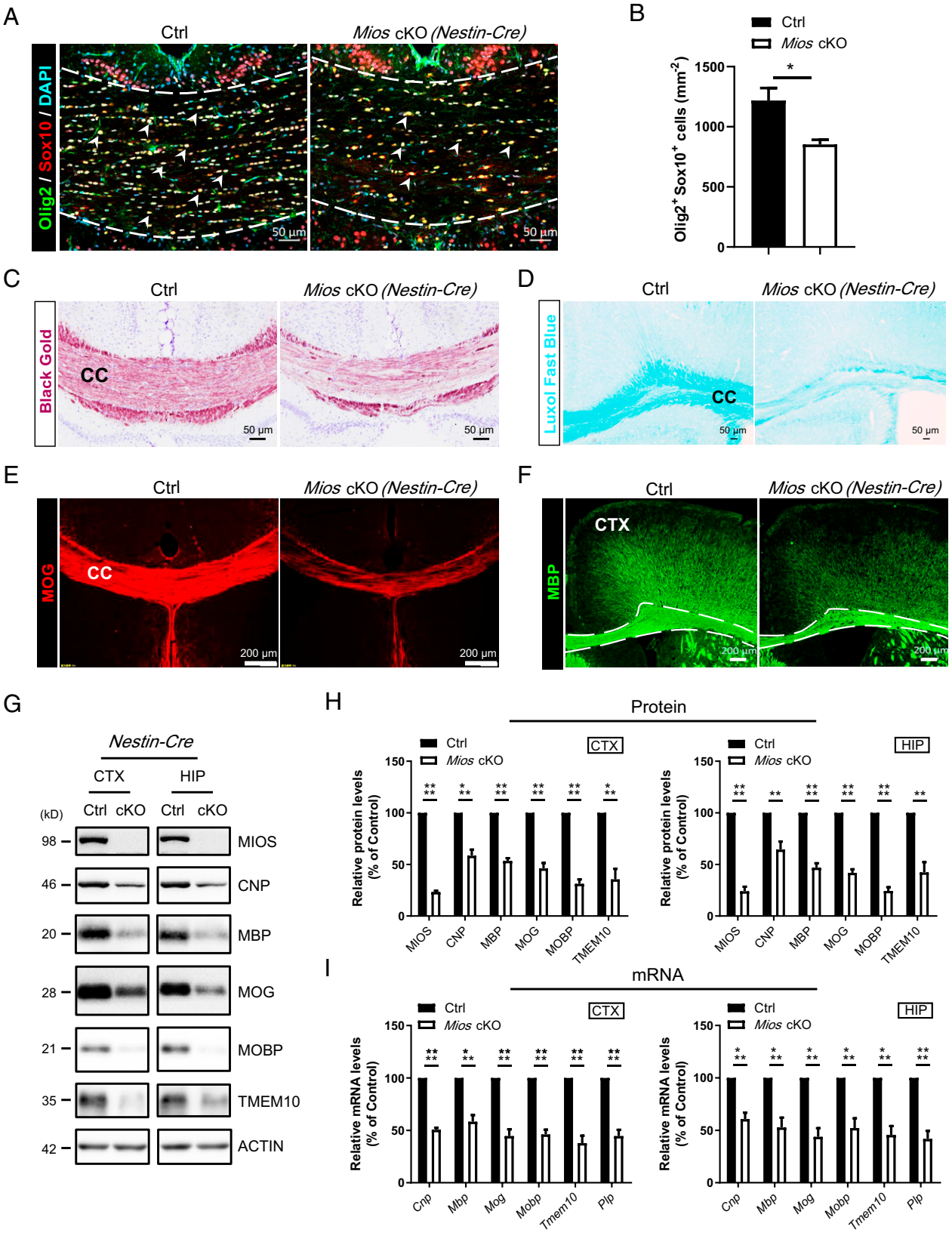

Fig. 1. Myelination deficit in *Mios f/f; Nestin-Cre* cKO mice. (*A* and *B*) Immunostaining and quantitation of Olig2$^+$ Sox10$^+$ DAPI$^+$cells showing decreased oligodendrocyte number in the corpus callosum (CC) of the 3-wk *Mios f/f; Nestin-Cre* mouse. Arrowheads indicate Olig2$^+$ Sox10$^+$ cells ($n = 3$ pairs of mice). (*C*) Black Gold staining and (*D*) Luxol Fast Blue staining showing reduced staining in the CC of the 4-wk *Mios f/f; Nestin-Cre* mouse. (*E* and *F*) Reduced immunostaining of (*E*) MOG and (*F*) MBP in the CC and cerebral cortex (CTX) of the 4-wk *Mios f/f; Nestin-Cre* mouse. (Scale bars: *A*, *C*, and *D*, 50 μm; *E* and *F*, 200 μm.) (*G* and *H*) Western blots and quantifications (percentage of control [Ctrl]) showing reduced myelin proteins in the CTX and hippocampus (HIP) of the 6-wk *Mios f/f; Nestin-Cre* mouse ($n = 4$ pairs of mice). (*I*) qRT-PCR analysis showing decreased mRNA levels (percentage of Ctrl) of myelin genes in the CTX and HIP of the 6-wk *Mios f/f; Nestin-Cre* mouse ($n = 5$ pairs of mice). Data are represented as mean ± SEM and analyzed with the two-tailed unpaired Student's *t* test. *$P < 0.05$; **$P < 0.01$; ***$P < 0.001$; ****$P < 0.0001$.

in which *Mios* participated plays a general role in oligodendrocyte myelination in the brain.

Altered neuronal signaling pathways can also affect oligodendrocyte formation and myelination (32). To rule out a role of neuronal *Mios* expression in oligodendrocyte myelination, we genetically deleted *Mios* in neurons (*CamKII-Cre*) (29). Consistent with the abundant expression of *Mios* in neurons, *CamKII-Cre*-mediated deletion of *Mios* in neurons significantly reduced Mios in the brain (*SI Appendix*, Fig. S4 *A* and *B*). However, axonal growth and myelination were preserved (*SI Appendix*, Fig. S4 *C*–*G*). These findings suggest that neuronal *Mios* does not contribute to the regulation of brain myelination and enhance the point that the myelination deficit in the *Mios* cKO mouse is an oligodendrocyte-intrinsic effect.

***Mios* cKO Affects the Proliferation and Differentiation of OPCs.** Now that the myelination deficit of the *Mios* cKO mouse is an oligodendrocyte-intrinsic effect, we examined how the formation of the oligodendrocyte lineage is altered by *Mios* cKO in OPCs. Like *Mios f/f; Nestin-Cre* cKO, the *Mios f/f; Olig2-Cre* cKO mouse reduced the production of oligodendrocyte lineage cells ($Olig2^+$ $Sox10^+$) to a similar extent (Fig. 3 *A* and *B*), which is consistent with an oligodendrocyte-intrinsic role of Mios. *Mios* cKO does not affect the survival of oligodendrocytes; no increase in apoptosis of the oligodendrocyte lineage was noted in the brain or in cultures (*SI Appendix*, Fig. S5 *A* and *B*).

To better understand how *Mios* deletion reduces the formation of the oligodendrocyte lineage, we assessed the numbers of OPCs and differentiated oligodendrocytes in the *Mios f/f; Olig2-Cre* mouse by immunostaining. During the early postnatal stage, OPCs proliferate and form a stable pool, with OPCs evenly distributed in the brain and maintained throughout the adult brain (33). In the rodent brain, the great majority of oligodendrocyte lineage cells are formed during the first 6 wk after birth. We found that the numbers of both OPCs ($Olig2^+$ $PDGFR\alpha^+$) and differentiated oligodendrocytes ($Olig2^+$ $CC1^+$) were reduced in the brain of the *Mios f/f; Olig2-Cre* mouse (Fig. 3 *C*–*F*). The reduction in the number of differentiated oligodendrocytes is consistent with the finding obtained by cumulative 5-bromo-2'-dexoyuridine (BrdU) labeling to examine the production of differentiated oligodendrocytes from proliferative OPCs. The number of differentiated oligodendrocytes ($BrdU^+$ $CC1^+$) derived from the initially BrdU-labeled OPC pool was reduced in the corpus callosum of the *Mios* cKO mouse (Fig. 3 *G*–*I*). Acute BrdU labeling (2 h) in the early postnatal mice revealed that the number of proliferative cells of the oligodendrocyte lineage ($BrdU^+$ $Olig2^+$) was reduced in the *Mios* cKO mouse (Fig. 3 *J*–*L*), suggesting that Mios plays a role in the regulation of OPCs proliferation. DNA replication is a key event in cell division; altered S-phase length is characteristic of dysregulated cell proliferation (34). We assessed the duration of the DNA synthesis phase (Ts) of OPCs through sequentially injecting BrdU and EdU (5-ethynyl-2'-deoxyuridine). The data we obtained show that the Ts of the *Mios* cKO OPCs was prolonged (Fig. 3 *M*–*P*). To further assess the cell cycle progression of *Mios* cKO OPCs in the corpus callosum, we performed BrdU and Ki67 (antigen identified by monoclonal antibody Ki67) double labeling. $BrdU^+$ $Ki67^+$ colabeling indicates OPCs in the cycling mode, whereas $BrdU^+$ $Ki67^-$ OPCs are out of the cell cycle. We found that the proportion of $BrdU^+Ki67^+$ OPCs in the corpus callosum of the *Mios* cKO brain was significantly higher than that of control brain (Fig. 3 *Q*–*S*). This result is consistent with the increase in Ts (duration of S phase) of the *Mios* cKO OPCs and indicates that the cell cycle progression of *Mios* cKO OPCs was impaired. In further support of the notion that *Mios* cKO impairs the progression of S phase, S phase–related proteins Cyclin A2 and CDK2 (35) were reduced in the *Mios* cKO OPCs (*SI Appendix*, Fig. S5 *C* and *D*). The increased OPCs in cycling mode suggest that the cell cycle exit of the *Mios* cKO OPCs would be delayed, which could reduce the differentiation of OPCs to postmitotic oligodendrocytes expressing the CC1 marker.

***Mios* Transgene Restores Oligodendrocyte Myelination in *Mios* cKO Mouse.** To further validate that the loss of Mios function is responsible for the deficit in oligodendrocyte formation and myelination, we generated *Mios* conditional transgenic (cTG) mouse using *Rosa26* knock in (*SI Appendix*, Fig. S6*A*) and performed genetic rescue of the *Mios* cKO mouse. First, we validated the *Cre*-dependent expression of the *Mios* transgene. Expression of the *Mios* transgene tagged with hemagglutinin (HA) was readily detected in the brain by western blotting (*SI Appendix*, Fig. S6*B*). Also, the *Mios* transgene expression did not alter myelin protein expressions in the brain (*SI Appendix*, Fig. S6*B*). We then expressed one copy of the *Mios* transgene in the *Mios* cKO mouse under the control of *Olig2-Cre*. The *Mios* transgene compensated for the loss of *Mios* expression from the endogenous loci and restored oligodendrocyte linage (*SI Appendix*, Fig. S6 *C* and *D*). Black Gold staining and Luxol Fast Blue staining each showed comparable staining intensity in the corpus callosum of control and *Mios* cKO; cTG mice (*SI Appendix*, Fig. S6 *E* and *F*). In addition, the *Mios* transgene restored the expressions of most myelin proteins to >90% of the control level (*SI Appendix*, Fig. S6 *G*–*I*). These studies validate that the phenotype of oligodendrocyte myelination in the *Mios* cKO brain is indeed due to the loss of Mios function.

Mios Participates in Maintaining mTORC1 Activity in a Cell Type–Specific Manner. Mios, a lysosomal protein (22), participates in amino acid signaling to mTORC1 (22, 27). Mios colabeling with the lysosomal marker Lamp2 shows that Mios is primarily localized to the lysosomes in OPCs (*SI Appendix*, Fig. S7*A*); no apparent staining was detected in the nucleus. To examine the molecular mechanism by which *Mios* deletion impairs the oligodendrocyte lineage, we first assessed the effect of *Mios* deletion on mTORC1 in the brain of the *Mios f/f; Nestin-Cre* mouse. Surprisingly, western blotting to assess mTORC1 activity in the brain of the *Mios* cKO mouse showed almost comparable levels of mTORC1 activity–related phosphorylated substrates, including phosphorylated S6 kinase (p-S6K; Thr-389), phosphorylated S6 (p-S6; Ser-240/244), and p-S6 (Ser-235/236) (*SI Appendix*, Fig. S7 *B* and *C*). In the adult brain, the bulk of mTORC1 activity is contributed by neurons; therefore, we differentiated neuronal and oligodendroglia mTORC1 activity by p-S6 staining. We found that all neurons ($NeuN^+$) in the cortex are p-S6 $(Ser\text{-}240/244)^+$ in both control and *Mios f/f; Nestin-Cre* mice (*SI Appendix*, Fig. S7 *D* and *E*). Therefore, we further quantified the fluorescence intensity of p-S6 $(Ser\text{-}240/244)^+$ and found that the intensity was comparable between the *Mios* cKO and control mice (*SI Appendix*, Fig. S7*F*). To further validate the effect of the *Mios* cKO on developing neurons, we assessed mTORC1 activity of the embryonic cerebrum by western blotting and found no reduction in mTORC1 activity in the *Mios* cKO brain where Mios reduction was apparent (*SI Appendix*, Fig. S7 *G* and *H*).

In glial cells, the basal mTORC1 activity is much lower but readily detectable in the oligodendrocyte lineage by p-S6 staining. We then examined oligodendroglial mTORC1 activity in the *Mios f/f; Olig2-Cre* mouse. We found that the numbers of p-S6 $(Ser\text{-}240/244)^+$ and p-S6 $(Ser\text{-}235/236)^+$ oligodendrocyte lineage cells ($Olig2^+$) were significantly reduced in the corpus callosum of the *Mios f/f; Olig2-Cre* mouse (Fig. 4 *A* and *B* and *SI Appendix*, Fig. S6*I*). Meanwhile, we assessed mTORC1 activity in OPC cultures derived from the *Mios f/f; Olig2-Cre* mouse. Western blotting showed that the amounts of phosphorylated p-S6K and p-S6 were reduced in *Mios* cKO OPC

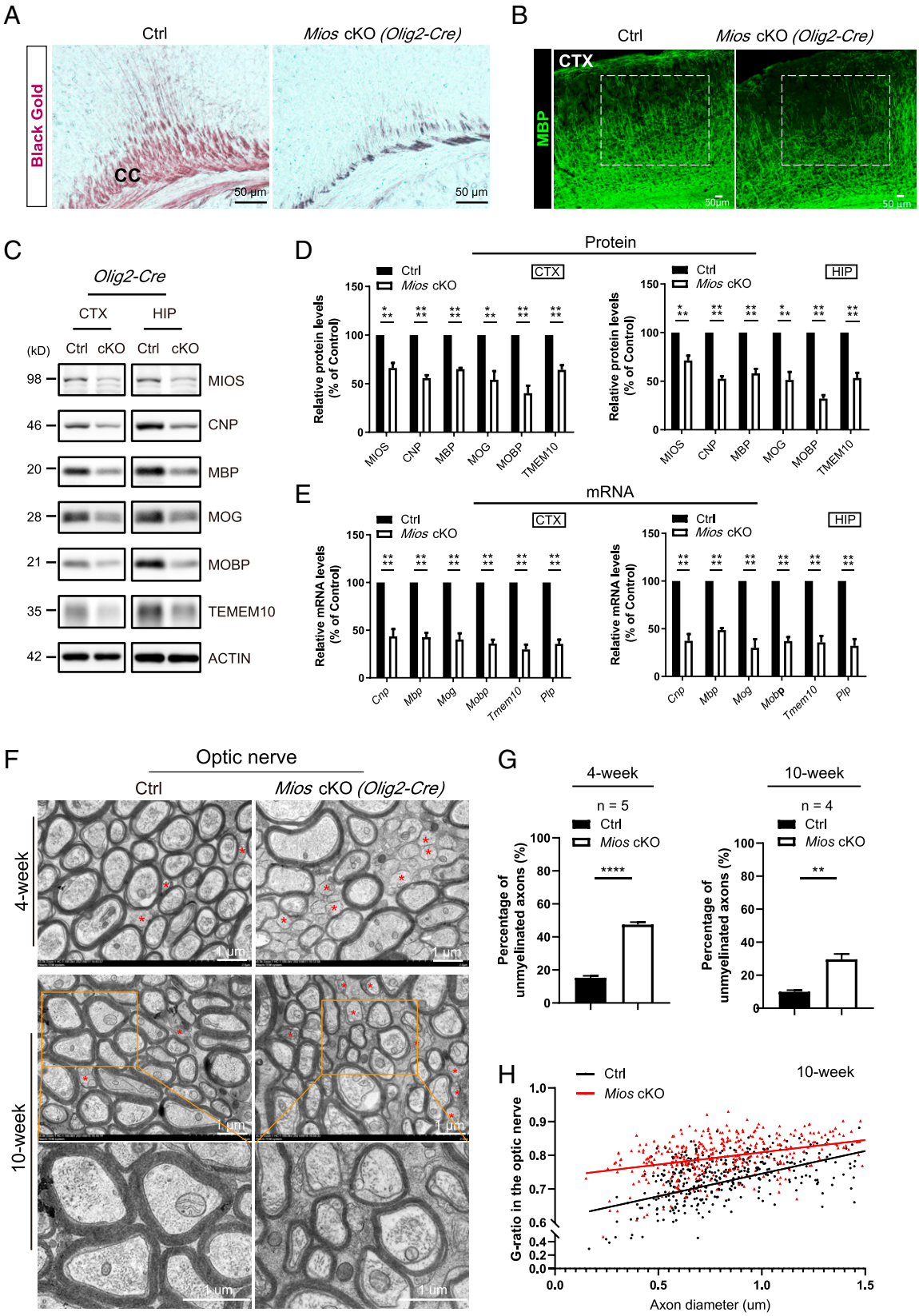

Fig. 2. Oligodendrocyte-intrinsic *Mios* regulates myelination in the central nervous system (CNS). (*A*) Black Gold staining showing decreased myelin staining in the corpus callosum (CC) of the 4-wk *Mios f/f; Olig2-Cre* mouse. (*B*) Immunostaining showing decreased MBP staining in the cerebral cortex (CTX; boxed area) of the 4-wk *Mios f/f; Olig2-Cre* mouse. (*C* and *D*) Western blots and quantifications (percentage of control [Ctrl]) showing reduced myelin proteins in the CTX and hippocampus (HIP) of the 6-wk *Mios f/f; Olig2-Cre* mouse ($n = 4$ pairs of mice). (*E*) qRT-PCR showing decreased mRNA levels (percentage of Ctrl) of myelin protein genes in the CTX and HIP of the 6-wk *Mios f/f; Olig2-Cre* mouse ($n = 5$ pairs of mice). (*F*) EM of the optic nerves from 4- and 10-wk *Mios f/f; Olig2-Cre* mice. Red asterisks indicate unmyelinated axons. (Scale bars: *A* and *B*, 50 μm; *F*, 1 μm.) (*G*) Quantification of unmyelinated axons in *F* showing reduced myelination in 4- and 10-wk *Mios f/f; Olig2-Cre* mice (*n* is the numbers of pairs of mice as indicated). (*H*) The g ratio of myelinated axons in the optic nerves from 10-wk Ctrl and *Mios f/f; Olig2-Cre* mice ($n = 3$ pairs of mice). Data are represented as mean ± SEM and analyzed with the two-tailed unpaired Student's *t* test. $^{**}P < 0.01$; $^{***}P < 0.001$; $^{****}P < 0.0001$.

cultures (Fig. 4 *C* and *D*), indicative of reduced mTORC1 activity in OPCs. Then, we asked if the *Mios* cKO renders OPCs unresponsive to the change of amino acid availability by examining how these cultured OPCs would respond to amino acid starvation/refeeding. We used culture medium that lacked arginine (Arg) and leucine (Leu) to starve cultured OPCs because these two amino acids have been reported to potentiate mTORC1 activity through GATOR2 (23, 36–38). After 2 h of starvation, standard OPC culture medium was readded to cell cultures for 30 min. We found that wild-type (WT) control cultures responded to amino acid refeeding by increasing mTORC1 activity, whereas *Mios* cKO cultures did not (Fig. 4 *E* and *F*). Because cells respond to amino acid starvation normally by increasing the phosphorylated eukaryotic initiation factor 2α (p-eIF2α) to reduce protein synthesis (39), we assessed how p-eIF2α was altered by the loss of Mios function under amino acid starvation. While WT OPCs responded to amino acid starvation by increasing p-eIF2α, *Mios* cKO OPCs did not, suggesting that *Mios* cKO OPCs have lost their capacity of dynamically changing eIF2α phosphorylation status in response to amino acid availability (Fig. 4 *G* and *H*). All these results indicate that *Mios* cKO impairs mTORC1 activity of OPCs and their response to amino acid availability.

Brain Myelination Is Coregulated by Amino Acid and Growth Factor Signaling Pathways. Previous studies have established that the growth factor–activated AKT–TSC–Rheb–mTORC1 pathway plays a critical role in oligodendrocyte formation and myelination in the brain (6–11). Recent studies also indicate that GATOR2-mediated amino acid signaling coregulates with growth factor signaling the lysosomal translocation and activity of TSC–Rheb and thus, mTORC1 activation (40–42). Little is known about the coordinate regulation of brain myelination by growth factor and amino acid signaling pathways. We asked if enhancing growth factor–activated mTORC1 activity could rescue the myelination deficit in the brain by crossing the constitutively active *Rheb S16H* transgene into the *Mios* cKO mouse. The *Cre*-dependent expression of the Rheb rescues mTORC1 and myelination deficit in the *Rheb* cKO mouse (43). First, we validated that the expression of the *Rheb* transgene in the oligodendrocyte lineage did not accelerate or impair brain myelin protein expression (*SI Appendix*, Fig. S8*A*), unlike what we noted in the transgenic mice expressing *Rheb S16H* in neural stem cells (43). Then, we examined the *Mios* cKO mice expressing the *Rheb* transgene (*Mios* cKO; *Rheb* cTG). As suggested from the *Mio*/*TSC1* double mutation in *Drosophila* oocytes (28), the expression of the *Rheb* transgene restored mTORC1 activity in the oligodendrocyte lineage of the *Mios* cKO mice, with the proportion of p-S6$^+$ oligodendrocytes slightly exceeding the control level (Fig. 5 *A* and *B*) and the phosphorylation of mTORC1 substrates elevated in western blotting (*SI Appendix*, Fig. S8*B*). This finding, together with the finding that Mios/GATOR2 is not required in neurons for mTORC1 signaling, suggests that the cytosol to lysosome translocation of the mTORC1 complex is not dependent on amino acid signaling to GATOR2. Presumably, a certain amount of mTORC1 might be constitutively recruited to and retained on the lysosome, regardless of the amino acid availability or Rag deletion (40, 41). Even though mTORC1 was restored in the oligodendrocyte lineage by the *Rheb* transgene, the number of oligodendrocyte lineage cells was not improved (Fig. 5 *C* and *D*). Differentiated oligodendrocytes expressing CC1 marker were increased modestly by the *Rheb* transgene (Fig. 5 *E* and *F*), but the expressions of myelin genes were not improved at both mRNA and protein levels (Fig. 5 *G* and *H* and *SI Appendix*, Fig. S8*C*). Accordingly, the myelination deficit remained in the *Mios* cKO mouse with the *Rheb* transgene, as shown by Black Gold, Luxol Fast Blue, MBP staining, and EM (Fig. 5 *I–K* and *SI Appendix*, Fig. S8 *D* and *E*). This finding suggests the codependence of amino acid and growth factor signaling in oligodendrocyte formation and brain myelination, and the role of Mios/GATOR2-mediated amino acid signaling in oligodendrocytes goes beyond to mTORC1 (Fig. 6).

Discussion

GATOR2 in Oligodendrocyte Formation and Myelination. This study demonstrates that GATOR2-mediated amino acid sensing/signaling plays an important role in the formation of oligodendroglia and brain myelination, as illustrated in Fig. 6. We show that GATOR2's function in the oligodendrocyte lineage is disrupted as a result of the loss of its component Mios, which is consistent with the result of *Mio* deletion in *Drosophila* oocytes (22). Therefore, Mios deletion mimics a condition of amino acid insufficiency. Because amino acid availability is crucial for cell growth and proliferation and GATOR2 is critically positioned between cytosolic amino acid sensors for Leu and Arg (Sestrins and Castors) and GATOR1 in the amino acid signaling pathway (20, 23, 36), one would think that disrupting GATOR2 would severely affect neural stem cells during early embryonic development and therefore, could impact the formation of all types of neural cells (neurons, astrocytes, and oligodendrocytes). Surprisingly, loss of *Mios* in neural stem cells does not apparently affect the formation of astrocytes and neurons; the numbers and distributions of astrocytes and neurons were comparable between *Mios* cKO and normal control mice. Only the oligodendrocyte lineage was affected by *Mios* cKO. The role of *Mios* in the regulation of oligodendrocyte formation is oligodendrocyte intrinsic. Genetic deletion of *Mios* in OPCs reduced oligodendrocyte formation and recapitulated the myelination deficit noted in *Mios* deletion in neural stem cells, whereas deletion of *Mios* in neurons had no effect. The myelination deficit is widespread in the brain and persists to adulthood, which suggests a fundamental role of Mios/GATOR2 in developmental oligodendrocyte myelination. It remains to be seen if Mios plays a role in the maintenance of myelin. The hypomyelination in the *Mios* cKO mouse could be a result of reduced proliferation and differentiation of OPCs in the early postnatal stage. This early-stage proliferation is critical to the formation of a stable pool of OPCs that is maintained until old age in rodents (1, 33). Reduced proliferation of OPCs as a result of disruption of GATOR2 is consistent with the role of amino acid in the regulation of cell proliferation through cell cycle control (44, 45). We found that *Mios* deletion prolonged the length of the OPC cell cycle and increased the number of OPCs in the S phase, suggesting that GATOR2 regulates cell cycle progression. Altered cell cycle exit of OPCs could account for the reduced differentiation of OPCs to postmitotic mature oligodendrocytes that myelinate axons (hence, hypomyelination in brain). Future work should identify the roles of Mios in differentiated oligodendrocytes.

Earlier studies show that the amino acid stress sensor GCN2 kinase–mediated signaling is essential for oligodendrocyte development, survival, and myelin formation in the brain (46). Under amino acid deficiency, oligodendrocytes activate the GCN2 kinase to reduce general protein synthesis and nutrient and energy expenditure. Such reduction confers resistance to oligodendrocyte injury in amino acid stress (46). Studies suggest that GCN2-mediated amino acid stress sensing could be linked to amino acid signaling to mTORC1 via the Leu sensor Sestrin2 (47), which through Mios/GATOR2, transduces signals eventually to lysosomal Rag–GTPase/mTOR. The study of the zebrafish *RagA* mutant indicates that the lysosomal Rag–GTPase plays a role in the regulation of myelination involving the lysosomal transcription factor EB (TFEB) (48). Activated TFEB represses the expression of myelin genes (48). It is unknown if

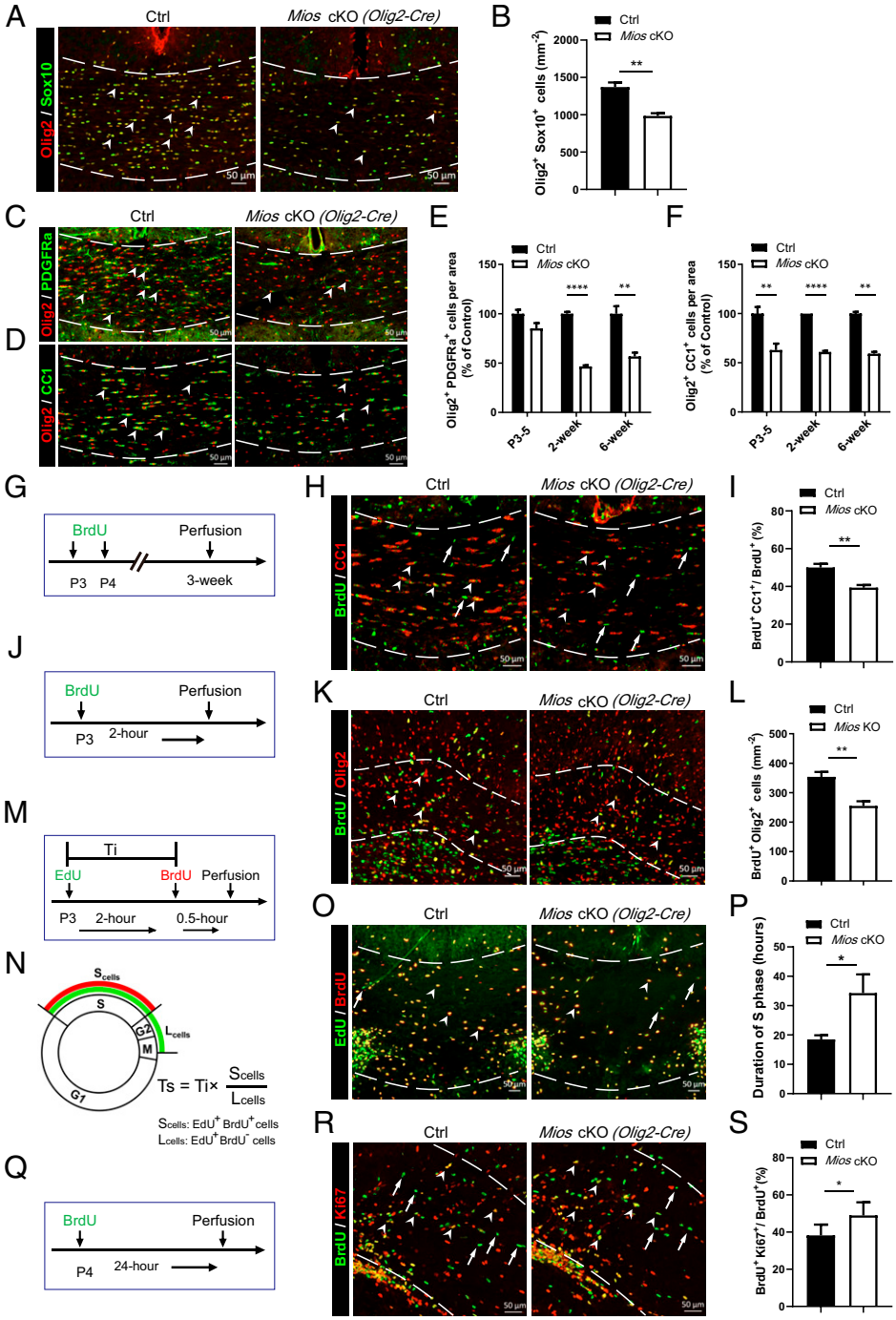

Fig. 3. Impairment in the proliferation and differentiation of *Mios* cKO OPCs. (*A* and *B*) Olig2 and Sox10 staining and quantitation showing decreased numbers of oligodendrocytes in the corpus callosum (CC) of 6-wk control (Ctrl) and *Mios f/f; Olig2-Cre* mice. Arrowheads indicate Olig2$^+$ Sox10$^+$ cells (n = 3 for Ctrl, n = 5 for *Mios* cKO). (*C–F*) Paired Olig2 staining with PDGFRα or CC1 and quantifications (percentage of Ctrl) showing the reduction in the numbers of OPCs and differentiated oligodendrocytes, respectively, in the CC of the *Mios f/f; Olig2-Cre* mouse. Arrowheads indicate Olig2$^+$ PDGFRα$^+$ and Olig2$^+$ CC1$^+$ cells (P3 to P5: n = 7 for Ctrl, n = 4 for *Mios* cKO; 2 wk: n = 4 for Ctrl, n = 3 for *Mios* cKO; 6 wk: n = 4 for Ctrl, n = 4 for *Mios* cKO). (*G–I*) BrdU and CC1 double labeling and quantification showing a decreased ratio of BrdU$^+$CC1$^+$/BrdU$^+$ in the CC of the 3-wk *Mios f/f; Olig2-Cre* mouse. Diagram showing the time points of BrdU administration and perfusion (*G*). Arrows indicate BrdU$^+$ cells, and arrowheads indicate BrdU$^+$ CC1$^+$ cells (n = 3 for Ctrl, n = 5 for *Mios* cKO). (*J–L*) Olig2 and BrdU staining and quantification showing the reduction in the number of proliferating OPCs in the CC of the P3 *Mios f/f; Olig2-Cre* mouse (*K* and *L*). (*J*) Illustration showing the time points of BrdU administration. Arrowheads indicate BrdU$^+$ Olig2$^+$ cells (*J*; n = 5 pairs of mice). (*M–P*) EdU and BrdU labeling showing cycling OPCs in the CC of the P3 *Mios f/f; Olig2-Cre* mouse (*O* and *P*), the experimental paradigm (*M*) illustrating the sequential labeling of OPCs with EdU and BrdU for the determination of the duration of S phase, and the calculation of Ts (*N*). Arrows indicate EdU$^+$ BrdU$^-$ cells, and arrowheads indicate EdU$^+$ BrdU$^+$ cells (n = 8 pairs of mice). (*Q–S*) BrdU and Ki67 double labeling and quantification showing the increased ratio of BrdU$^+$ Ki67$^+$/BrdU$^+$ in the CC of the P5 *Mios f/f; Olig2-Cre* mouse (*R* and *S*). Illustration (*Q*) showing the time points of BrdU administration and perfusion. Arrows indicate BrdU$^+$ cells, and arrowheads indicate BrdU$^+$ Ki67$^+$ cells (n = 5 for Ctrl, n = 6 for *Mios* cKO). S_{cells} are cells in S phase, and L_{cells} are cells exiting S phase. T_s is the duration of S phase, and T_i is the interval time of EdU and BrdU. Data are represented as mean ± SEM and analyzed with the two-tailed unpaired Student's t test. (Scale bars: *A*, *C*, *D*, *H*, *K*, *O*, and *R*, 50 μm.) *P < 0.05; **P < 0.01; ****P < 0.0001.

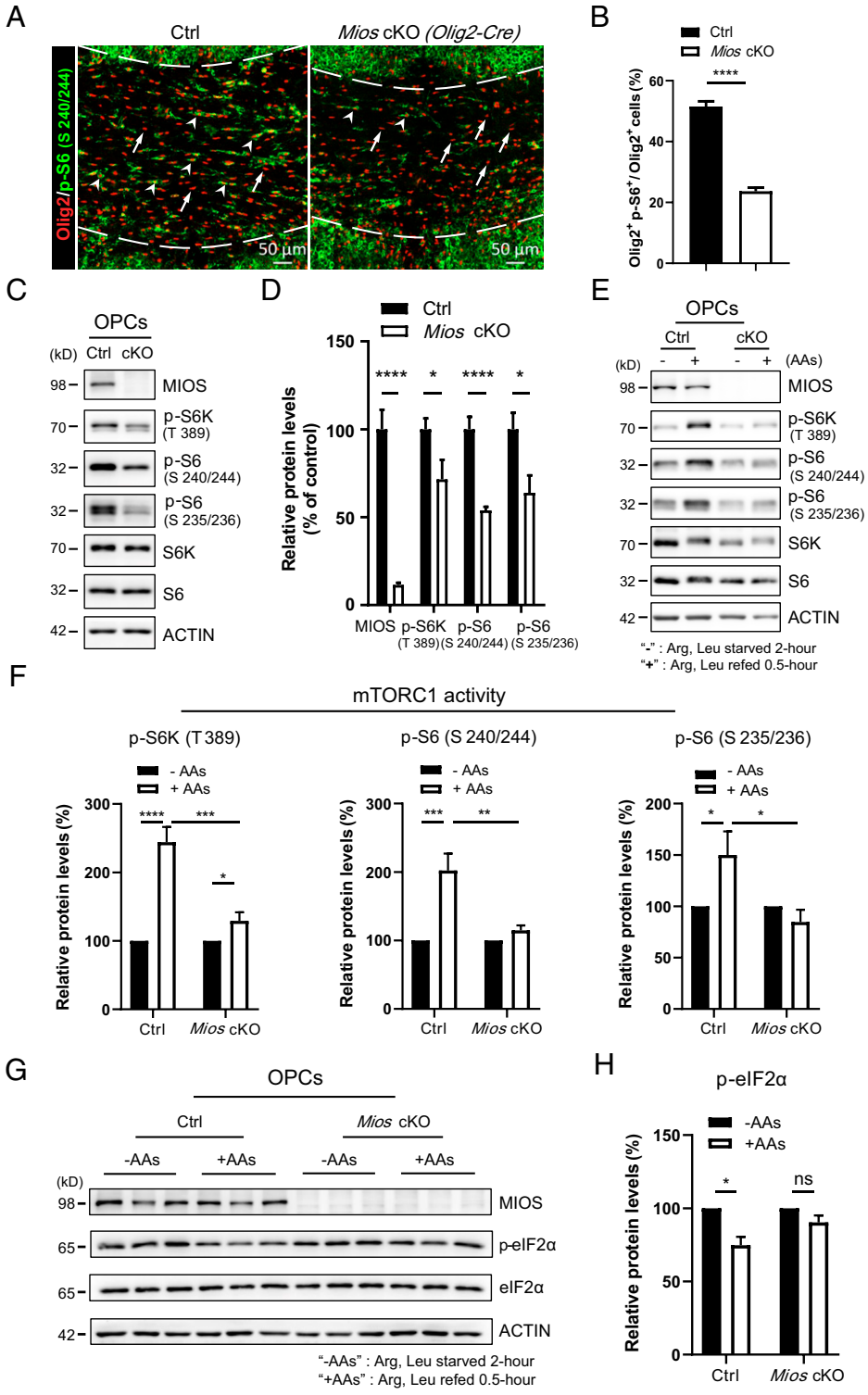

Fig. 4. Impaired oligodendendroglia amino acid signaling to mTORC1 in the *Mios* cKO lineage. (*A* and *B*) Olig2 and p-S6 (Ser-240/244) staining and quantification showing the decreased percentage of p-S6$^+$ Olig2$^+$/Olig2$^+$ in the corpus callosum of the P4 *Mios f/f; Olig2-Cre* mouse. Arrows indicate Olig2$^+$ cells, and arrowheads indicate Olig2$^+$ p-S6$^+$ cells (n = 5 pairs of mice). (Scale bars: *A*, 50 μm.) (*C* and *D*) Western blots and quantification of phosphorylated mTORC1 substrates (percentage of control [Ctrl]) showing reduced mTORC1 activity in cultured OPCs from the *Mios f/f; Olig2-Cre* mouse (n = 5 independent experiments with five batches of OPCs). (*E* and *F*) Western blots and quantifications of phosphorylated mTORC1 substrates (percentage of Ctrl) showing mTORC1 activity after amino acids starvation (−AAs) and refeeding (+AAs) in OPCs (n = 5 independent experiments with five batches of OPCs). (*G* and *H*) Western blots and quantification of the relative changes to p-eIF2α level normalized to total eIF2α in amino acid–starved and refed OPCs from Ctrl and *Mios* cKO mice (n = 6 independent experiments with six batches of OPCs). Data are represented as mean ± SEM and analyzed with the two-tailed unpaired Student's t test. *P < 0.05; **P < 0.01; ***P < 0.001; ****P < 0.0001.

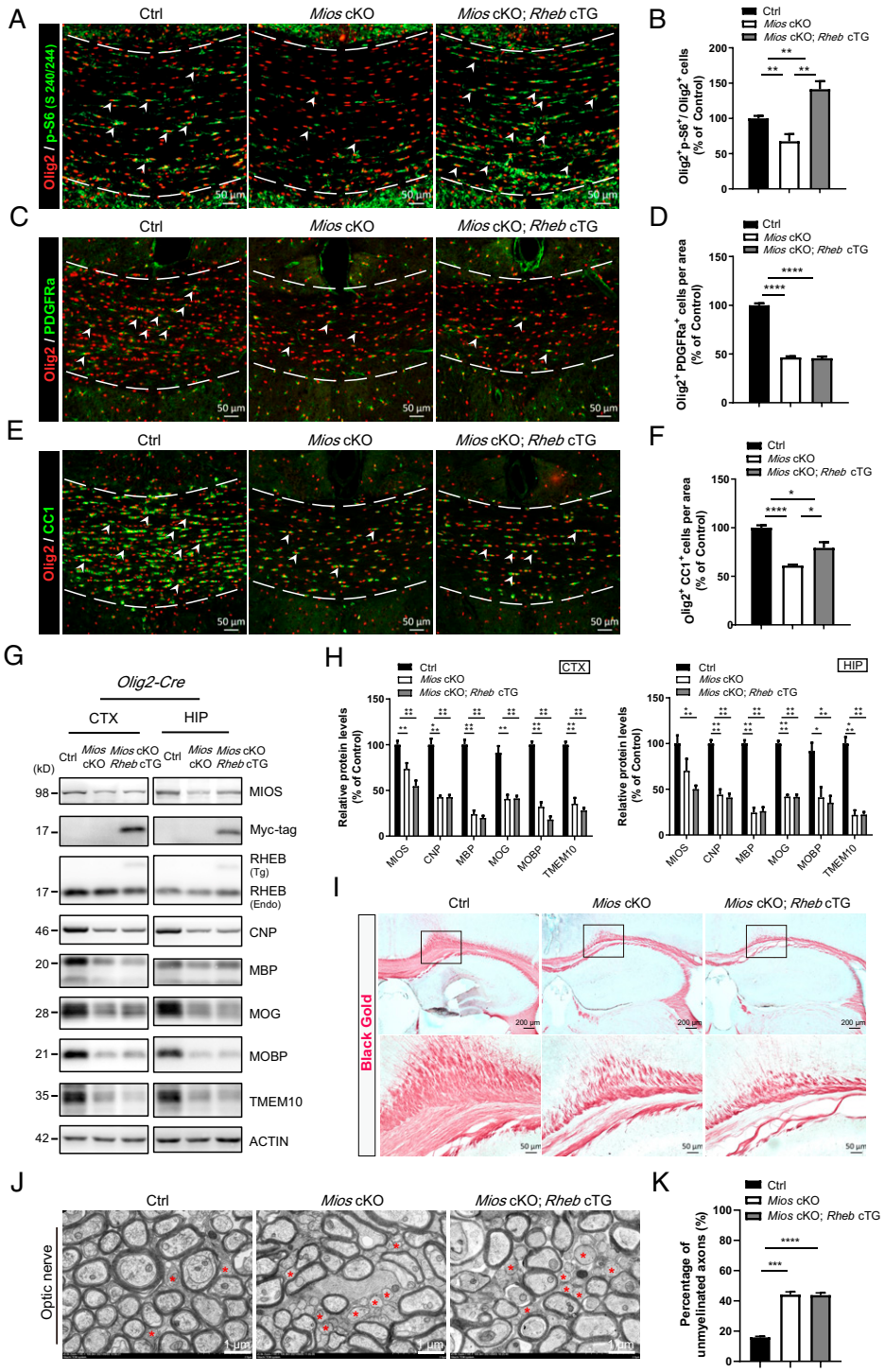

Fig. 5. Codependence of Mios/GATOR2-mediated amino acid signaling and growth factor signaling for proper myelination. (*A* and *B*) Olig2 and p-S6 (S240/244) staining and quantification (percentage of control [Ctrl]) showing restored mTORC1 activity in the corpus callosum (CC) of the 2-wk *Mios f/f; Rheb tg/+; Olig2-Cre* mouse by *Rheb* cTG. Arrowheads indicate Olig2$^+$ p-S6$^+$ cells (n = 7 for Ctrl, n = 4 for *Mios* cKO, n = 6 for *Mios* cKO; *Rheb* cTG). (*C* and *D*) Olig2 and PDGFRα staining and quantification (percentage of Ctrl) showing lower numbers of OPCs in the CC of 2-wk *Mios f/f; Olig2-Cre* and *Mios f/f; Rheb tg/+; Olig2-Cre* mice relative to the normal Ctrl mouse. Arrowheads indicate Olig2$^+$ PDGFRa$^+$ cells (n = 4 for Ctrl, n = 3 for *Mios* cKO, n = 3 for *Mios* cKO; *Rheb* cTG). (*E* and *F*) Olig2 and CC1 staining and quantification (percentage of Ctrl) showing decreased numbers of differentiated oligodendrocytes in the CC of the 2-wk *Mios f/f; Rheb tg/+; Olig2-Cre* mouse compared with Ctrl. Arrowheads indicate Olig2$^+$ CC1$^+$ cells (n = 4 for Ctrl, n = 3 for *Mios* cKO, n = 3 for *Mios* cKO; *Rheb* cTG). (*G* and *H*) Western blots and quantifications of myelin protein levels (percentage of Ctrl) showing reduction in the cerebral cortex (CTX) and hippocampus (HIP) of 6- to 8-wk *Mios f/f; Rheb tg/+; Olig2-Cre* and *Mios f/f; Olig2-Cre* mice (n = 9 for Ctrl, n = 3 for *Mios* cKO, n = 5 for *Mios* cKO; *Rheb* cTG). (*I*) Black Gold staining shows hypomyelination in the CC of 6-wk *Mios f/f; Rheb tg/+; Olig2-Cre* and *Mios f/f; Olig2-Cre* mice. (*J* and *K*) EM images and quantification showing comparable numbers of unmyelinated axons in the optic nerves from 4-wk *Mios f/f; Rheb tg/+; Olig2-Cre* and *Mios f/f; Olig2-Cre* mice (n = 3 pairs of mice). Data are represented as mean ± SEM and analyzed with One-way ANOVA and Tukey multiple comparison test. (Scale bars: *A*, *C*, *E*, and *I*, *Lower*, 50 μm; *I*, *Upper*, 200 μm; *J*, 1 μm.) *P < 0.05; **P < 0.01; ***P < 0.001; ****P < 0.0001.

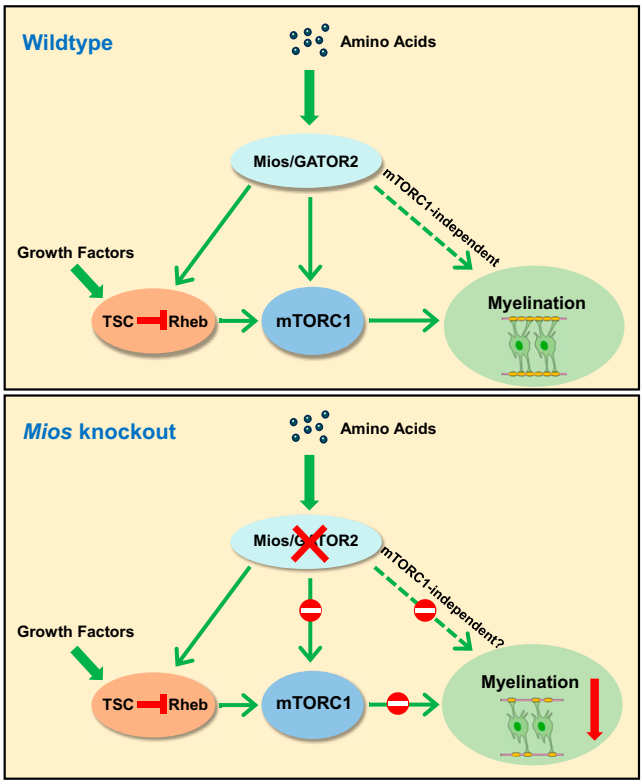

Fig. 6. A model for the role of the *Mios*/GATOR2 in brain myelination.

TFE3/TFEB family transcription factors are involved in Mios/GATOR2-regulated oligodendrocyte myelination.

Coordinate Regulation of Oligodendrocyte Myelination by Amino Acid and Growth Factor Signaling. Oligodendrocyte lineage formation and myelination are regulated by growth factor signaling through TSC and Rheb to mTORC1 (9–11, 43, 49). *Mios* deletion impairs mTORC1 activation in the oligodendrocyte lineage, suggesting that mTORC1 deficiency could contribute to the myelination deficit in brain, as indicated by mTORC1 deficiency mouse models (e.g., *Raptor* and *Rheb* cKO) (8, 9, 11, 43). The effect of *Mios* deletion on the oligodendrocyte lineage is different. Unlike *Raptor* and *Rheb* cKO, *Mios* cKO significantly reduces the number of OPCs, highlighting a critical role of GATOR2-mediated amino acid signaling in the regulation of the early expansion of OPCs.

GATOR2-regulated mTORC1 is involved in the regulation of cell mitosis and meiosis (50, 51) and oocyte development (28). Therefore, it seems that GATOR2 regulates oligodendrocyte biology through mTORC1. However, we found that mTORC1 deficit in the oligodendrocyte lineage can be rescued by the expression of the active *Rheb* transgene. Rescuing mTORC1 by *TSC1* knockdown in GATOR2 depletion oocytes corrects defects in oocyte development (28); however, restoring mTORC1 in the oligodendrocyte lineage of *Mios* cKO mice does not restore the oligodendrocyte lineage and myelination. These results suggest that Mios-containing GATOR2 engages an mTORC1-independent role in the control of the oligodendrocyte lineage or that *Mios* regulates oligodendrocyte biology independent of GATOR2. However, the GATOR2-independent role of Mios has not been reported.

GATOR2-mediated amino acid signaling intersects with growth factor signaling to regulate the lysosomal translocation and activation of TSC and Rheb (40, 41, 52), both of which are regulators of oligodendrocyte myelination (11, 53, 54). Now, we show that the GATOR2-mediated amino acid sensing/signaling pathway plays an important role in the formation of the oligodendrocyte lineage and brain myelination, suggesting that GATOR2-mediated amino acid signaling regulates oligodendrocyte lineage function in coordination with growth factor signaling (Fig. 6). The molecules involved in sensing different amino acids are found on the plasma membrane (55) and in the cytosol (23, 38, 56) and organelles, including mitochondria and lysosome (57, 58). Presumably, oligodendrocyte lineage cells could employ multiple mechanisms to sense the availability of different amino acids. This study of GATOR2 in the oligodendrocyte lineage will usher in more investigations into the roles of the complex amino acid–sensing mechanisms in oligodendrocyte biology.

Materials and Methods

Mice Strains. The generation of the *Mios f/f* mouse is described in *SI Appendix*. Additionally, the generation and characterization of *Rheb* knockout and transgenic mice have been previously described (43). *Nestin-Cre* (29), *Olig2-Cre* (31), and *CamKII-Cre* (59) mice were from The Jackson Laboratory.

Detection of Brain Myelination. Brain myelination was assessed by using multiple methods, which include Black Gold staining, Luxol Fast Blue staining, western blotting and immunostaining for myelin proteins, and EM to visualize myelinated axons in mouse brains. More details on the detection of myelination are provided in *SI Appendix*.

To quantify the myelination of axons, we performed EM of the optic nerves and corpus callosum from three to five mice per group. The percentage of unmyelinated axons was calculated based on the counts of at least 500 axons per mouse. The g ratio (the ratio of the diameter of the axon over the diameter of the entire myelinated axon) was calculated based on the measurements of 150 axons of the optic nerves per mouse with ImageJ. The two-tailed unpaired Student's *t* test was used for the statistical significance for two-group comparison, and one-way ANOVA and the Tukey test were used for multiple-group comparison. Measurements of the diameters of myelinated and unmyelinated axons in comparable electron microscope images were performed using ImageJ. The perimeter (c) of the axon was measured, and the diameter was calculated using the formula $d = c/2\Pi$. This analysis was done with three pairs of mice, with 500 axons per mouse analyzed.

Immunostaining Analysis of Neurons and Neuroglia. Standard immunostaining with anti-NeuN (neuronal nuclei) antibody was performed to assess the formation of neurons in the cortex and hippocampus of *Mios* cKO and control brains. To assess the formation of astrocytes, anti-GFAP (glial fibrillary acidic protein) staining was performed to quantify the number of astrocytes in the corpus callosum. To examine the oligodendrocyte lineage, anti-Olig2 and anti-Sox10 staining was performed to quantify the oligodendrocyte lineage cells in the corpus callosum of the brains. To differentiate OPCs and differentiated oligodendrocytes, we performed anti-PDGFRα and anti-CC1 staining, respectively. At least three comparable brain sections per mouse were included in each experiment, and three or more pairs of mice were examined for statistical analysis. The number of cells per area (millimeters squared) was counted using ImageJ. For $Olig2^+PDGFR\alpha^+$ cells and $Olig2^+CC1^+$ cells, cell numbers per area in the corpus callosum of *Mios* cKO were normalized to control mice of comparable ages. The statistical significance was assessed using the two-tailed unpaired Student's *t* test for two-group comparison and one-way ANOVA and the Tukey test for multiple-group comparison.

OPC Proliferation and Differentiation with BrdU and EdU Single or Dual Labeling. BrdU and EdU labeling was performed to analyze the proliferation and differentiation of OPCs. BrdU (Sigma; 19-160) and EdU (Invitrogen; C10337) were dissolved in phosphate-buffered saline (PBS) in 5 mg/mL and always preserved at −20 °C from light. Acute BrdU labeling (2 h) was performed by intraperitoneally (i.p.) injecting BrdU (100 μg) for labeling proliferative OPCs in the early postnatal (P3 [postnatal day 3] to P4) mice. The brains were isolated and fixed with 4% PFA (paraformaldehyde) at 4 °C for 48 h, followed by sequential immersion in 20 and 30% sucrose for cryopreservation. Frozen brains were sectioned at 40-mm thickness. Brain cryosections were processed with heat-induced antigen retrieval for 10 min at 95 °C in sodium citrate buffer (10 mM, pH 6). Sections were washed three times and stained with rat anti-BrdU (Abcam; ab6326; 1:500) and rabbit anti-Olig2 (Millipore; AB9610; 1:200) antibodies. The number of $BrdU^+$ $Olig2^+$ OPCs per area (millimeters squared) in the corpus callosum of mice was counted.

Cumulative BrdU labeling was performed by i.p. injecting P3 and P4 mice with 100 μg BrdU for 2 consecutive days, and then, at 3 wk, the brain samples were harvested after perfusion with cold PBS and 4% PFA (as described above). After cryopreservation, 16-mm brain sections were cut and stained with antibodies of rat anti-BrdU and mouse anti-CC1 (Sigma; OP80; 1:100). The index indicative of the differentiation capacity was calculated as the percentage of the $BrdU^+$ $CC1^+$ cells divided by total $BrdU^+$ cells in the corpus callosum.

BrdU and EdU dual labeling was performed to measure the cell cycle length (Ts) of OPCs in the early postnatal stage mice. EdU (100 μg) was administered to neonatal mice (P3 to P4) through i.p. injection, which was followed by i.p. injection of BrdU (100 μg) 2 h later. Thirty minutes after the BrdU injection, the mouse brain was isolated and fixed at 4 °C as described above. The brains were collected for immunostaining with antioligodendrocyte lineage antibody to visualize BrdU- and EdU-labeled OPCs or differentiated oligodendrocytes. EdU was detected according to Click-iT EdU imaging kits' instructions (Invitrogen; C10337). The formula for calculating Ts is illustrated in Fig. 3*N*.

BrdU and Ki67 double labeling was performed to examine the cell cycle exit of OPCs. BrdU (100 μg i.p.) was injected to P4 mice to assess proliferating OPCs; 24 h later, brain tissues were processed and stained with rat anti-BrdU and rabbit anti-Ki67 (Abcam; ab16667; 1:500) antibodies to identify OPCs that are $BrdU^+$ $Ki67^+$ or $BrdU^+$ $Ki67^-$. For the assessment of the cell cycle exit, the percentage of the $BrdU^+Ki67^+$ cells relative to $BrdU^+$ cells was calculated as an index of cell cycle exit.

The statistical significance was assessed using the two-tailed unpaired Student's *t* test.

Amino Acids Starvation and Refeeding to OPC Cultures. The method of setting up OPC cultures is described in *SI Appendix*. Amino acid starvation and refeeding experiments were conducted based on the previous study (27). Primary OPCs cultures were washed once with Dulbecco's PBS and then, incubated with Arg- and Leu-free medium (custom made) for 2 h, which was supplemented with 2% B-27 serum-free supplement, 10 ng/mL PDGF-AA (platelet-derived growth factor-AA), 10 ng/mL bFGF (basic fibroblast growth factor), 1 ng/mL NT3 (neurotrophin-3), and penicillin–streptomycin–glutamine. For refeeding, the medium was then replaced with routine OPC medium (DMEM/F-12 (Dulbecco's modified Eagle medium/nutrient mixture F-12) and additives mentioned above); 30 min later, the cells were harvested for western blotting.

Detection of mTORC1 Activation. mTORC1 activation was assessed by detecting the phosphorylation of its canonical substrates, such as S6 kinase and its phosphorylated substrate, the ribosomal protein S6. We used western blotting to detect p-S6K (Thr-389; CST 9234), p-S6 (Ser-240/244; CST 2215), and p-S6 (Ser-235/236; CST 2211) in mouse brains and OPC cultures. We also performed immunostaining with p-S6 (Ser-240/244; CST 2215) and p-S6 (Ser-235/236; CST 62016) antibodies to assess mTORC1 activity of different cell types in the brain. The antibody dilutions were as follows: p-S6K at 1:2,000 for western blotting, p-S6 (Ser-240/244; CST 2215) at 1:1,000 for western blotting and 1:500 for immunostaining, and p-S6 (Ser-235/236; CST 2211) at 1:1,000 for western blotting and 1:500 for immunostaining (CST 62016). For quantifying the mTORC1 activity changes detected by western blotting, the relative amount of the phosphorylated amount vs. its total amount of the individual protein in the brain or cell cultures under indicated conditions was quantified using ImageJ. For quantifying cellular mTORC1 activity detected by immunostaining, the ratio of $Olig2^+$ $p\text{-}S6^+$ cells divided by total $Olig2^+$ cells in the corpus callosum and the ratio of $NeuN^+$ $p\text{-}S6^+$ cells divided by total $NeuN^+$ cells in the cortex were computed. Fluorescence intensity of p-S6 in neurons was also calculated with Zen software. The statistical difference was assessed using the two-tailed unpaired Student's *t* test.

Data Availability. All study data are included in the article and/or *SI Appendix*.

ACKNOWLEDGMENTS. We thank Southern University of Science and Technology (SUSTech) Core Research Facilities for assistance with EM and the SUSTech Animal Core Facility for animal care. This work was supported by Shenzhen Innovation Committee of Science and Technology Grants ZDSYS20200811144002008 (to the Shenzhen Key Laboratory of Gene Regulation and Systems Biology) and 2019193984 (to B.X.); National Natural Science Foundation of China Grants 30800311 (to M.C.), 31970773 (to B.X.), and 31530042 (to B.X.); and Shenzhen–Hong Kong Institute of Brain Science–Shenzhen Fundamental Research Institutions Grant 2021SHIBS0002.

1. D. E. Bergles, W. D. Richardson, Oligodendrocyte development and plasticity. *Cold Spring Harb. Perspect. Biol.* **8**, a020453 (2015).
2. K. A. Nave, H. Ehrenreich, Myelination and oligodendrocyte functions in psychiatric diseases. *JAMA Psychiatry* **71**, 582–584 (2014).
3. R. D. Fields, White matter in learning, cognition and psychiatric disorders. *Trends Neurosci.* **31**, 361–370 (2008).
4. B. Elbaz, B. Popko, Molecular control of oligodendrocyte development. *Trends Neurosci.* **42**, 263–277 (2019).
5. J. M. Levine, R. Reynolds, J. W. Fawcett, The oligodendrocyte precursor cell in health and disease. *Trends Neurosci.* **24**, 39–47 (2001).
6. S. P. Narayanan, A. I. Flores, F. Wang, W. B. Macklin, Akt signals through the mammalian target of rapamycin pathway to regulate CNS myelination. *J. Neurosci.* **29**, 6860–6870 (2009).
7. K. K. Bercury, W. B. Macklin, Dynamics and mechanisms of CNS myelination. *Dev. Cell* **32**, 447–458 (2015).
8. F. Lebrun-Julien *et al.*, Balanced mTORC1 activity in oligodendrocytes is required for accurate CNS myelination. *J. Neurosci.* **34**, 8432–8448 (2014).
9. K. K. Bercury *et al.*, Conditional ablation of raptor or rictor has differential impact on oligodendrocyte differentiation and CNS myelination. *J. Neurosci.* **34**, 4466–4480 (2014).
10. S. E. Wahl, L. E. McLane, K. K. Bercury, W. B. Macklin, T. L. Wood, Mammalian target of rapamycin promotes oligodendrocyte differentiation, initiation and extent of CNS myelination. *J. Neurosci.* **34**, 4453–4465 (2014).
11. Y. Zou *et al.*, Oligodendrocyte precursor cell-intrinsic effect of Rheb1 controls differentiation and mediates mTORC1-dependent myelination in brain. *J. Neurosci.* **34**, 15764–15778 (2014).
12. R. A. Saxton, D. M. Sabatini, mTOR signaling in growth, metabolism, and disease. *Cell* **168**, 960–976 (2017).
13. V. Hietakangas, S. M. Cohen, Regulation of tissue growth through nutrient sensing. *Annu. Rev. Genet.* **43**, 389–410 (2009).
14. A. M. Hosios *et al.*, Amino acids rather than glucose account for the majority of cell mass in proliferating mammalian cells. *Dev. Cell* **36**, 540–549 (2016).
15. L. Y. Cheng *et al.*, Anaplastic lymphoma kinase spares organ growth during nutrient restriction in Drosophila. *Cell* **146**, 435–447 (2011).
16. S. Deoni, D. Dean III, S. Joelson, J. O'Regan, N. Schneider, Early nutrition influences developmental myelination and cognition in infants and young children. *Neuroimage* **178**, 649–659 (2018).
17. K. J. Condon, D. M. Sabatini, Nutrient regulation of mTORC1 at a glance. *J. Cell Sci.* **132**, jcs222570 (2019).
18. S. Dokudovskaya *et al.*, A conserved coatomer-related complex containing Sec13 and Seh1 dynamically associates with the vacuole in *Saccharomyces cerevisiae*. *Mol Cell Proteomics* **10**, M110 006478 (2011).
19. R. L. Wolfson, D. M. Sabatini, The dawn of the age of amino acid sensors for the mTORC1 pathway. *Cell Metab.* **26**, 301–309 (2017).
20. L. Chantranupong *et al.*, The Sestrins interact with GATOR2 to negatively regulate the amino-acid-sensing pathway upstream of mTORC1. *Cell Rep.* **9**, 1–8 (2014).
21. A. Parmigiani *et al.*, Sestrins inhibit mTORC1 kinase activation through the GATOR complex. *Cell Rep.* **9**, 1281–1291 (2014).
22. W. Cai, Y. Wei, M. Jarnik, J. Reich, M. A. Lilly, The GATOR2 component Wdr24 regulates TORC1 activity and lysosome function. *PLoS Genet.* **12**, e1006036 (2016).
23. L. Chantranupong *et al.*, The CASTOR proteins are arginine sensors for the mTORC1 pathway. *Cell* **165**, 153–164 (2016).
24. Y. Sancak *et al.*, The Rag GTPases bind raptor and mediate amino acid signaling to mTORC1. *Science* **320**, 1496–1501 (2008).
25. Y. Sancak *et al.*, Ragulator-Rag complex targets mTORC1 to the lysosomal surface and is necessary for its activation by amino acids. *Cell* **141**, 290–303 (2010).
26. D. J. Kwiatkowski, B. D. Manning, Tuberous sclerosis: A GAP at the crossroads of multiple signaling pathways. *Hum. Mol. Genet.* **14 Spec No. 2**, R251–R258 (2005).
27. L. Bar-Peled *et al.*, A Tumor suppressor complex with GAP activity for the Rag GTPases that signal amino acid sufficiency to mTORC1. *Science* **340**, 1100–1106 (2013).
28. Y. Wei *et al.*, TORC1 regulators Iml1/GATOR1 and GATOR2 control meiotic entry and oocyte development in Drosophila. *Proc. Natl. Acad. Sci. U.S.A.* **111**, E5670–E5677 (2014).
29. F. Tronche *et al.*, Disruption of the glucocorticoid receptor gene in the nervous system results in reduced anxiety. *Nat. Genet.* **23**, 99–103 (1999).
30. L. E. Rivers *et al.*, PDGFRA/NG2 glia generate myelinating oligodendrocytes and piriform projection neurons in adult mice. *Nat. Neurosci.* **11**, 1392–1401 (2008).
31. U. Schüller *et al.*, Acquisition of granule neuron precursor identity is a critical determinant of progenitor cell competence to form Shh-induced medulloblastoma. *Cancer Cell* **14**, 123–134 (2008).
32. C. Stritt *et al.*, Paracrine control of oligodendrocyte differentiation by SRF-directed neuronal gene expression. *Nat. Neurosci.* **12**, 418–427 (2009).
33. E. G. Hughes, S. H. Kang, M. Fukaya, D. E. Bergles, Oligodendrocyte progenitors balance growth with self-repulsion to achieve homeostasis in the adult brain. *Nat. Neurosci.* **16**, 668–676 (2013).
34. J. Nordman, T. L. Orr-Weaver, Regulation of DNA replication during development. *Development* **139**, 455–464 (2012).
35. J. Rosenblatt, Y. Gu, D. O. Morgan, Human cyclin-dependent kinase 2 is activated during the S and G2 phases of the cell cycle and associates with cyclin A. *Proc. Natl. Acad. Sci. U.S.A.* **89**, 2824–2828 (1992).
36. J. S. Kim *et al.*, Sestrin2 inhibits mTORC1 through modulation of GATOR complexes. *Sci. Rep.* **5**, 9502 (2015).

37. R. A. Saxton, L. Chantranupong, K. E. Knockenhauer, T. U. Schwartz, D. M. Sabatini, Mechanism of arginine sensing by CASTOR1 upstream of mTORC1. *Nature* **536**, 229–233 (2016).
38. R. L. Wolfson *et al.*, Sestrin2 is a leucine sensor for the mTORC1 pathway. *Science* **351**, 43–48 (2016).
39. R. C. Wek, B. M. Jackson, A. G. Hinnebusch, Juxtaposition of domains homologous to protein kinases and histidyl-tRNA synthetases in GCN2 protein suggests a mechanism for coupling GCN4 expression to amino acid availability. *Proc. Natl. Acad. Sci. U.S.A.* **86**, 4579–4583 (1989).
40. S. Yang *et al.*, The rag GTPase regulates the dynamic behavior of TSC downstream of both amino acid and growth factor restriction. *Dev. Cell* **55**, 272–288.e5 (2020).
41. C. Demetriades, N. Doumpas, A. A. Teleman, Regulation of TORC1 in response to amino acid starvation via lysosomal recruitment of TSC2. *Cell* **156**, 786–799 (2014).
42. S. Menon *et al.*, Spatial control of the TSC complex integrates insulin and nutrient regulation of mTORC1 at the lysosome. *Cell* **156**, 771–785 (2014).
43. J. Zou *et al.*, Rheb1 is required for mTORC1 and myelination in postnatal brain development. *Dev. Cell* **20**, 97–108 (2011).
44. C. J. Nelsen *et al.*, Amino acids regulate hepatocyte proliferation through modulation of cyclin D1 expression. *J. Biol. Chem.* **278**, 25853–25858 (2003).
45. A. Nowosad *et al.*, p27 controls Ragulator and mTOR activity in amino acid-deprived cells to regulate the autophagy-lysosomal pathway and coordinate cell cycle and cell growth. *Nat. Cell Biol.* **22**, 1076–1090 (2020).
46. P. She *et al.*, General control nonderepressible 2 (GCN2) kinase protects oligodendrocytes and white matter during branched-chain amino acid deficiency in mice. *J. Biol. Chem.* **288**, 31250–31260 (2013).
47. J. Ye *et al.*, GCN2 sustains mTORC1 suppression upon amino acid deprivation by inducing Sestrin2. *Genes Dev.* **29**, 2331–2336 (2015).
48. A. M. Meireles *et al.*, The lysosomal transcription factor TFEB represses myelination downstream of the rag-ragulator complex. *Dev. Cell* **47**, 319–330.e5 (2018).
49. B. A. Barres, M. C. Raff, Control of oligodendrocyte number in the developing rat optic nerve. *Neuron* **12**, 935–942 (1994).
50. M. Platani, I. Samejima, K. Samejima, M. T. Kanemaki, W. C. Earnshaw, Seh1 targets GATOR2 and Nup153 to mitotic chromosomes. *J. Cell Sci.* **131**, jcs213140 (2018).
51. M. Platani, L. Trinkle-Mulcahy, M. Porter, A. A. Jeyaprakash, W. C. Earnshaw, Mio depletion links mTOR regulation to Aurora A and Plk1 activation at mitotic centrosomes. *J. Cell Biol.* **210**, 45–62 (2015).
52. Y. Yao *et al.*, Amino acids enhance polyubiquitination of Rheb and its binding to mTORC1 by blocking lysosomal ATXN3 deubiquitinase activity. *Mol. Cell* **80**, 437–451.e6 (2020).
53. E. Ercan *et al.*, Neuronal CTGF/CCN2 negatively regulates myelination in a mouse model of tuberous sclerosis complex. *J. Exp. Med.* **214**, 681–697 (2017).
54. L. Meikle *et al.*, A mouse model of tuberous sclerosis: Neuronal loss of Tsc1 causes dysplastic and ectopic neurons, reduced myelination, seizure activity, and limited survival. *J. Neurosci.* **27**, 5546–5558 (2007).
55. E. M. Wauson *et al.*, The G protein-coupled taste receptor T1R1/T1R3 regulates mTORC1 and autophagy. *Mol. Cell* **47**, 851–862 (2012).
56. J. M. Han *et al.*, Leucyl-tRNA synthetase is an intracellular leucine sensor for the mTORC1-signaling pathway. *Cell* **149**, 410–424 (2012).
57. R. Zoncu *et al.*, mTORC1 senses lysosomal amino acids through an inside-out mechanism that requires the vacuolar H(+)-ATPase. *Science* **334**, 678–683 (2011).
58. S. H. Kim *et al.*, Mitochondrial threonyl-tRNA synthetase TARS2 is required for threonine-sensitive mTORC1 activation. *Mol. Cell* **81**, 398–407.e4 (2021).
59. E. Casanova *et al.*, A CamKIIalpha iCre BAC allows brain-specific gene inactivation. *Genesis* **31**, 37–42 (2001).